

Electronic Supplementary Information (ESI)

Ionic Hydrogen Bond Effects on Polyelectrolyte Brushes beyond the Hydronium and Hydroxide Ions

Jian Zhang,^{ab} Siyuan Xu,^a Hengguo Jin,^a and Guangming Liu^{*a}

^aHefei National Laboratory for Physical Sciences at the Microscale, Key Laboratory of Surface and Interface Chemistry and Energy Catalysis of Anhui Higher Education Institutes, Department of Chemical Physics, University of Science and Technology of China, No. 96, Jinzhai Road, Hefei, P. R. China 230026.

^bCollege of Material and Textile Engineering, Jiaxing University, Jiaxing, 314001, P. R. China

Materials and Methods

Materials. 2-(Methacryloyloxy)ethyltrimethylammonium chloride (METAC) (75 wt% in H₂O, Aladdin) was used after purification with a basic alumina column. Sodium methacrylate (MANa) (99%, Aladdin), sodium hydroxide ($\geq 96\%$, Sinopharm), and ethylene diamine tetracetic acid (EDTA) ($\geq 99.5\%$, Sinopharm) were used as received. Copper(I) bromide (CuBr) was prepared from CuBr₂ by reacting with sodium sulfite. ω -Mercaptoundecyl bromoisobutyrate (MUBB) was synthesized according to the procedure reported previously.^{S1} Ethyl 2-bromoisobutyrate (2-EBiB, 98%, Aldrich), 2, 2'-bipyridyl (BPy, 98%), sodium methanesulfonate (CH₃SO₃Na, 97%, TCI), formaldehyde-sodium bisulfite adduct (HOCH₂SO₃Na, $> 98\%$, Aladdin), ethanol ($\geq 99.7\%$, Sinopharm), methanol ($\geq 99.9\%$, Sigma Aldrich), sodium chloride (NaCl, 99.99%, Aladdin), and guanidinium chloride (GdmCl, 99%, Aladdin) were all used as received. The water used was purified by filtration through a Millipore Gradient system after pre-distillation, giving a resistivity of 18.2 M Ω cm. The phosphate buffer (PB) solutions with an ionic strength of 20 mM were employed as the background solutions to prepare the salt solutions with different pH values.

Preparation of Polyelectrolyte Brushes. The substrates coated with a gold layer were cleaned with the piranha solution at ~ 60 °C for ~ 10 min, followed by a rinse with water and ethanol and a dry with N₂. Afterwards, the substrates were immersed in a 5 mM MUBB ethanol solution for ~ 24 h at room temperature to modify the substrates with initiators. The PMETAC and PMANa brushes were prepared by using a surface-initiated atom-transfer radical polymerization (SI-ATRP) method.^{S2,S3} Typically, for the synthesis of the PMETAC brush, METAC (~ 6 g), BPy (~ 27 mg), and 2-EBiB (~ 9 mg) were dissolved in a methanol/water mixture [4:1 (v/v), ~ 20 mL]. The solvent mixture was then degassed by a freeze-pump-thaw process for three cycles and backfilled with N₂. Subsequently, the initiator-modified substrates and CuBr (~ 25 mg) were added to a flask under the protection of N₂ to initiate the polymerization at room temperature. After the polymerization was completed, the substrates grafted with the PMETAC brush were rinsed with water and methanol in sequence, followed by soaking

the substrates in methanol overnight to remove the unreacted monomer and the adsorbed ligand.

For the preparation of the PMANa brush, the substrates modified with initiators were placed in a dry flask and back-filled with N₂ three times. Meanwhile, MANa (~ 2.12 g), CuBr (~ 29 mg), CuBr₂ (~ 9 mg), and BPy (~ 78 mg) were added to another flask. A ~ 4 mL of water with a pH of ~ 9 adjusted by NaOH was bubbled with N₂ for at least 30 min, and then transferred into the flask containing MANa. The solution mixture was stirred under the protection of N₂ for ~ 10 min at room temperature, then a viscous brown solution was observed. Afterwards, the solution mixture was transferred into the flask containing the substrates to start the polymerization at room temperature. After the polymerization was conducted for ~ 15 min, the substrates were taken out of the solution, followed by a rinse with water and a gentle sonication in a 0.1 M EDTA solution for ~ 1 to 2 min. Finally, the PMANa brush was rinsed with water and ethanol, and dried with N₂. The dry thickness of both PMETAC and PMANa brushes was ~ 20 nm, as determined by a spectroscopic ellipsometry (M-2000 V, J. A. Woollam) in air.

In situ Combination of Quartz Crystal Microbalance with Dissipation (QCM-D) and Spectroscopic Ellipsometry Measurements. The ionic hydrogen bond effects on polyelectrolyte brushes were studied using a combination of QCM-D and spectroscopic ellipsometry.^{S4,S5} The quartz crystal sensor has a fundamental resonance frequency (f_0) of ~ 5 MHz and a mass sensitivity constant (C) of 17.7 ng·cm⁻²·Hz⁻¹.^{S6} Under vacuum or in air, if the adsorbed layer on the sensor surface is rigid, evenly distributed, and much thinner than the quartz crystal, then the frequency change (Δf) is related to the mass change (Δm) of the adsorbed layer and the overtone number ($n = 1, 3, 5...$) by the Sauerbrey equation^{S7}

$$\Delta m = -\frac{\rho_q l_q}{f_o} \frac{\Delta f}{n} = -C \frac{\Delta f}{n} \quad (\text{S1})$$

where ρ_q is the density of the quartz crystal and l_q is the thickness of the quartz crystal. The dissipation factor (D) is defined by^{S8}

$$D = \frac{E_d}{2\pi E_s} \quad (S2)$$

where E_d and E_s are the energy dissipated during one oscillation and the energy stored in the oscillating system, respectively. In this study, all of the results obtained were from the measurements of the frequency and dissipation factor at the third overtone ($n = 3$), and all of the experiments were conducted at ~ 25 °C. As the frequency and dissipation factor were also influenced by the changes in solution density and viscosity during solution exchange, the Δf and ΔD of the polyelectrolyte brushes were extracted by subtracting the background response of the blank resonator and with the values of Δf and ΔD in water as the reference.

In the spectroscopic ellipsometry measurements, the phase difference (Δ) is related to Ψ by the following equation^{S9}

$$\tan(\Psi)e^{i\Delta} = \frac{R_p}{R_s} \quad (S3)$$

where $\tan(\Psi)$ is the amplitude ratio of the reflection coefficient of p-polarized light (R_p) to that of s-polarized light (R_s). Both the dry and wet thicknesses of polyelectrolyte brushes were determined by treating the brushes as a single Cauchy layer. With this model, the index of refraction (n) of the brushes followed the Cauchy dispersion equation of $n = A + (B/\lambda^2) + (C/\lambda^4)$,^{S10} where λ was the wavelength of incident light and the three parameters of A , B , and C could be obtained by using the software CompleteEASE to fit the ellipsometric data. The optical properties of the resonator's surface gold layer obtained from the ellipsometry measurements were fixed during modeling of the brushes in the determination of the dry and wet thicknesses of the polyelectrolyte brushes.

Other Measurements. A contact angle goniometer (CAM 200, KSV) was employed to measure the water contact angle (WCA) and underwater oil (n-hexadecane) contact angle (OCA) on the surfaces of polyelectrolyte brushes at ~ 25 °C. The pendant bubble contact angle method was applied to determine the WCA on the surfaces of

polyelectrolyte brushes. The sum-frequency generation vibrational spectroscopy (SFG-VS) experiments of the PMETAC brush (dry thickness ~ 20 nm) were carried out at ~ 25 °C. The measurements of UV spectra were carried out on a UNICO 2802PCS UV/visible spectrophotometer at ~ 25 °C.

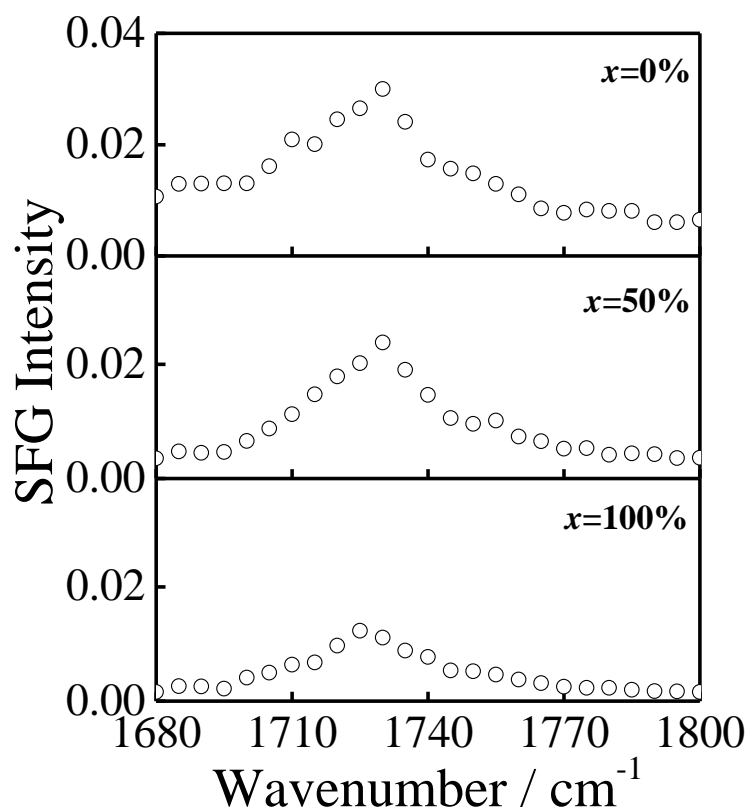


Fig. S1. The ppp SFG spectra of the PMETAC brush in the frequency range of 1680 to 1800 cm^{-1} as a function of the mole fraction of $\text{HOCH}_2\text{SO}_3^-$ (x) at a salt concentration of 50 mM of the salt mixtures.

In Fig. S1, the peak at $\sim 1730 \text{ cm}^{-1}$ is assigned to the C=O stretching of the $-\text{C}(=\text{O})\text{OR}$ group of PMETAC. The red shift of this peak from 1730 to 1724 cm^{-1} with increasing mole fraction of $\text{HOCH}_2\text{SO}_3^-$ (x) of the salt mixtures indicates that more hydrogen bonds are formed between the bound $\text{HOCH}_2\text{SO}_3^-$ counterions and the carbonyl groups of grafted chains as x increases.

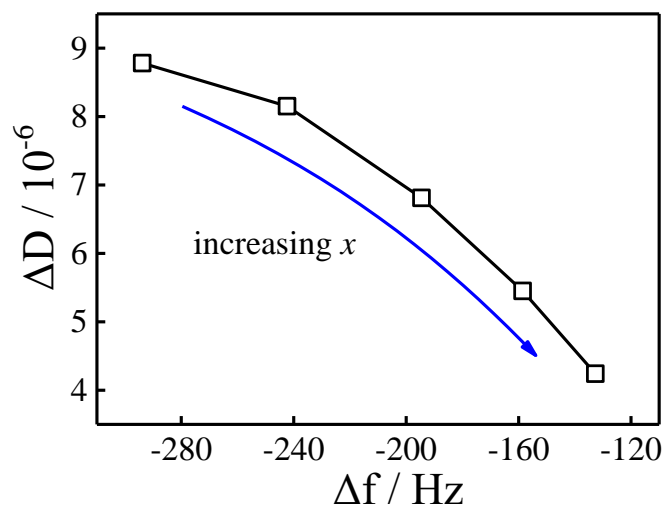


Fig. S2. ΔD versus Δf of the PMETAC brush as a function of the mole fraction of $\text{HOCH}_2\text{SO}_3^-$ (x) at a salt concentration of 50 mM of the $\text{HOCH}_2\text{SO}_3\text{Na}-\text{CH}_3\text{SO}_3\text{Na}$ mixtures.

In Fig. S2, the slope of the ΔD - Δf plot decreases from -0.012 in the low x region to -0.047 in the high x region, indicating that the ionic hydrogen bonding has a stronger influence on the stiffness but a weaker effect on the hydration of the PMETAC brush with increasing x . This could be attributed to the weak cooperativity between the changes in hydration and stiffness of the brush during the formation of hydrogen bonds between the bound $\text{HOCH}_2\text{SO}_3^-$ counterions and the grafted chains.^{S11}

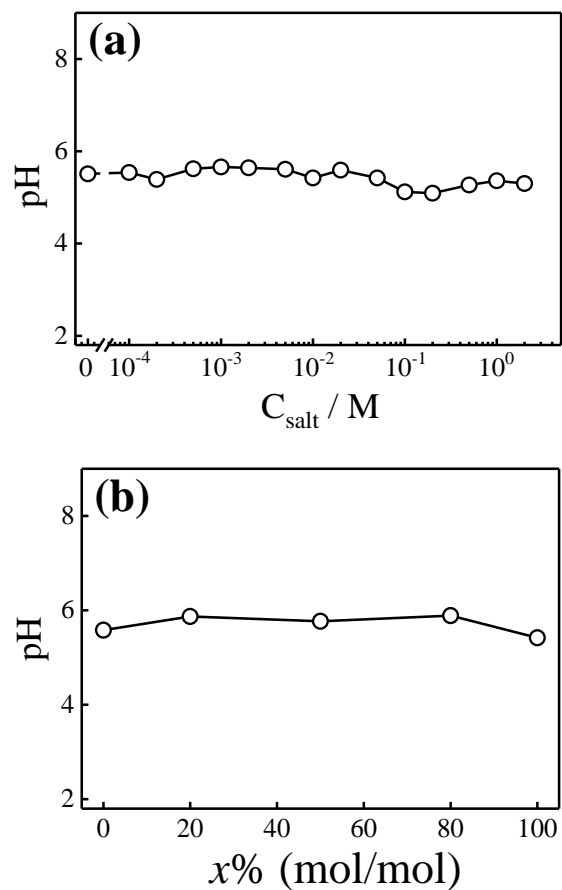


Fig. S3. (a) The salt concentration (C_{salt}) dependence of pH of the $\text{HOCH}_2\text{SO}_3\text{Na}$ solutions. (b) pH of the $\text{HOCH}_2\text{SO}_3\text{Na}$ - $\text{CH}_3\text{SO}_3\text{Na}$ mixtures with a salt concentration of 50 mM as a function of the mole fraction of $\text{HOCH}_2\text{SO}_3\text{Na}$ (x).

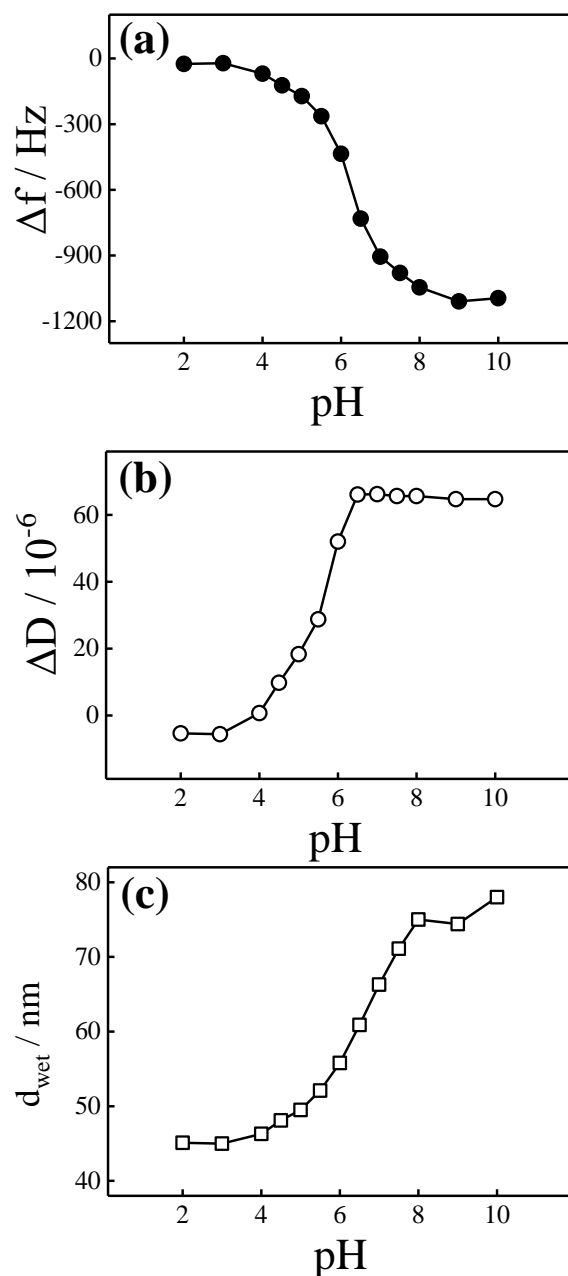


Fig. S4. (a) Δf of the PMANa brush as a function of pH. (b) ΔD of the PMANa brush as a function of pH. (c) d_{wet} of the PMANa brush as a function of pH. Here, the pH is controlled by the 20 mM PB solutions in the absence of external NaCl or GdmCl.

In Fig. S4a, Δf decreases with increasing pH, indicating a strengthening hydration of the PMANa brush due to the increasing degree of charging of the brush. Meanwhile, in Fig. S4b and S4c, ΔD and d_{wet} increase as the pH is increased, suggesting that the increasing degree of charging of the grafted chains leads to a softer and more swollen PMANa brush.

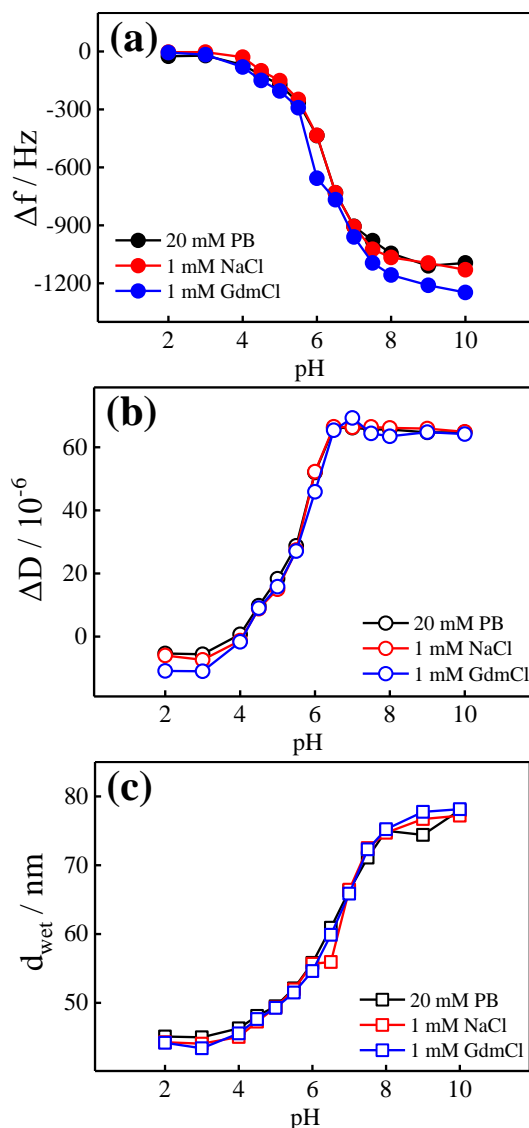


Fig. S5. (a) Δf of the PMANa brush as a function of pH in the either absence or presence of 1 mM NaCl or GdmCl. (b) ΔD of the PMANa brush as a function of pH in the either absence or presence of 1 mM NaCl or GdmCl. (c) d_{wet} of the PMANa brush as a function of pH in the either absence or presence of 1 mM NaCl or GdmCl. Here, the pH is controlled by the 20 mM PB solutions.

According to the previous study,^{S4} the strength of ionic hydrogen bond effects is influenced by the competitive binding of counterions to the PMANa brush between Na^+ and Gdm^+ . In the presence of 1 mM GdmCl, the concentration of Gdm^+ is much lower than that of Na^+ from the PB solutions. Thus, the addition of 1 mM GdmCl has no obvious influences on the pH response of the PMANa brush, as shown in Fig. S5.

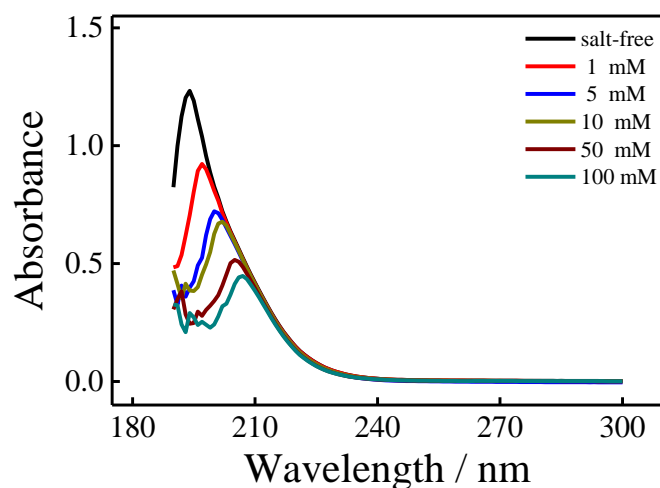


Fig. S6. The UV spectra of 0.25 mg mL⁻¹ PMANa solution ($M_w \sim 9.5 \times 10^3$ g/mol, PDI ~ 1.7) with a phosphate buffer (pH ~ 8.0 , 20 mM) as the background solution in the range of wavelength from 190 to 300 nm as a function of the concentration of GdmCl.

In Fig. S6, the peak at ~ 191 nm is assigned to the π - π^* transition of the $-\text{C}=\text{O}$ group of PMANa. The red shift of this peak with increasing concentration of GdmCl indicates that more hydrogen bonds are formed between the Gdm^+ counterions and the $-\text{C}=\text{O}$ groups as the concentration of GdmCl increases. Thus, at a given concentration of GdmCl, more ionic hydrogen bonds would be formed in the PMANa brush with increasing pH due to the increasing degree of charging of the grafted chains.

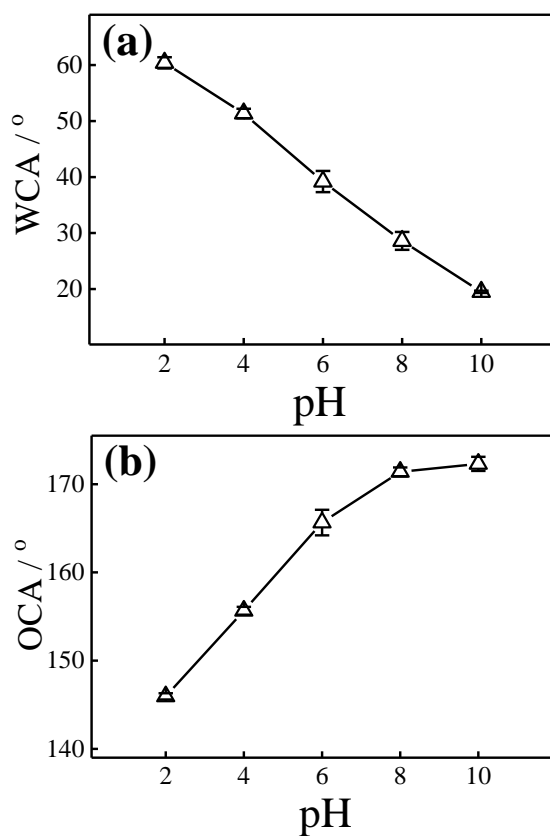


Fig. S7. (a) WCA on the surface of the PMANa brush as a function of pH in the absence of external NaCl or GdmCl. (b) OCA on the surface of the PMANa brush as a function of pH in the absence of external NaCl or GdmCl.

References

- S1 D. M. Jones, A. A. Brown and W. T. S. Huck, *Langmuir*, 2002, **18**, 1265-1269.
- S2 S. Edmondson, V. L. Osborne and W. T. S. Huck, *Chem. Soc. Rev.*, 2004, **33**, 14-22.
- S3 M. G. Santonicola, G. W. D. Groot, M. Memesa, A. Meszyńska and G. J. Vancso, *Langmuir*, 2010, **26**, 17513-17519.
- S4 J. Zhang, R. Kou and G. M. Liu, *Langmuir*, 2017, **33**, 6838-6845.
- S5 J. J. I. Ramos and S. E. Moya, *Macromol. Rapid Commun.*, 2011, **32**, 1972-1978.
- S6 F. Höök, B. Kasemo, T. Nylander, C. Fant, K. Sott and H. Elwing, *Anal. Chem.*, 2001, **73**, 5796-5804.
- S7 G. Sauerbrey, *Z. Phys.*, 1959, **155**, 206-212.
- S8 M. Rodahl, F. Höök, A. Krozer, P. Brzezinski and B. Kasemo, *Rev. Sci. Instrum.*, 1995, **66**, 3924-3930.
- S9 H. Tompkins and E. A. Irene, *Handbook of Ellipsometry*, William Andrew, 2005.
- S10 K. Hinrichs and K. J. Eichhorn, *Ellipsometry of Functional Organic Surfaces and Films*, Springer Berlin Heidelberg, 2014.
- S11 G. M. Liu, G. Z. Zhang, *J. Phys. Chem., B.*, 2005, **109**, 743-747.